

1 Article

2 **Single crystal growth and superconducting properties**
3 **of Antimony Substituted $\text{NdO}_{0.7}\text{F}_{0.3}\text{BiS}_2$** 4 **Satshi Demura*, Satoshi Otsuki, Yuita Fujisawa and Hideaki Sakata**

5 Tokyo University of Science, Department of Physics, Shinjuku-ku, Tokyo 162-8601, Japan

6 Correspondence: demura@rs.tus.ac.jp; Tel:+81-3-3260-4271(2223)

7 **Abstract:** Antimony (Sb) Substitution less than 10 % is examined on a single crystal of a layered
8 superconductor $\text{NdO}_{0.7}\text{F}_{0.3}\text{BiS}_2$. Superconducting transition temperature of the substituted samples
9 decreases with increasing Sb concentration. A lattice constant along the c axis showed a large
10 decrease compared with that along the a axis. Since in-plane chemical pressure monotonically
11 decreases with increasing Sb concentration, the suppression of the superconductivity is well
12 described in terms of the decrease in in-plane chemical pressure.

13 **Keywords:** BiS_2 -based superconductor; Flux growth; Layered structure; Superconducting
14 Properties; Magnetic susceptibility measurement; Electrical resistivity measurement

16 **1. Introduction**

17 New layered BiS_2 -based superconductors $\text{Bi}_4\text{O}_4\text{S}_3$ and $\text{Ln}(\text{O},\text{F})\text{BiS}_2$ ($\text{Ln}=\text{La}, \text{Ce}, \text{Pr}, \text{Nd}, \text{Sm}, \text{Yb}$
18 and Bi) have been reported [1-9]. Although a superconducting transition temperature (T_c) of
19 $\text{Ln}(\text{O},\text{F})\text{BiS}_2$ is around 4 K, T_c is increased by introduction of a lattice strain. One of the ways to
20 introduce the lattice strain is a partial element substitution with a different ionic radius into Ln , Bi or
21 S site [12-17]. The strain introduced by the partial element substitution in these crystals is called as
22 chemical pressure. For instance, when Selenium (Se) is partially substituted with Sulfur (S) in the
23 superconducting layer in $\text{La}(\text{O},\text{F})\text{BiS}_2$, T_c and a superconducting volume fraction increase [10-11]. The
24 substitution into Ln site in the block layer for smaller lanthanide ion also increases T_c [12-14]. The
25 increase in T_c by the element substitution is correlated with in-plane chemical pressure defined by
26 Mizuguchi: T_c increases with increasing in-plane chemical pressure [18]. The change in T_c by the
27 element substitution of Ln or S sites is described by the increase of in-plane chemical pressure. On
28 the other hand, it is not known whether the change in T_c is understood by in-plane chemical pressure
29 when an element is partially substituted into Bi site.

30 Here, we report on an examination of a substitution of Antimony (Sb) ion less than 10 % into
31 $\text{NdO}_{0.7}\text{F}_{0.3}\text{BiS}_2$. Since the Sb ion has a same valence as that of Bi ion, an effect of the chemical pressure
32 can be investigated without the effect of the carrier concentration. We found that the lattice constant
33 along the c and a axis of Sb substituted samples decreased. On the other hand, superconductivity was
34 suppressed by the Sb substitution. This suppression by the Sb substitution can be explained by the
35 change of the in-plane chemical pressure.

36 **2. Experiment**

37 $\text{NdO}_{0.7}\text{F}_{0.3}\text{Bi}_{1-x}\text{Sb}_x\text{S}_2$ ($x=0.01-0.10$) single crystals were synthesized using a CsCl/KCl flux method
38 in an evacuated quartz tubes [19, 20]. Powders of Nd_2S_3 , Bi_2O_3 , Bi_2S_3 , Sb_2S_3 and BiF_3 with Bi grains
39 were used as a starting material. The Bi_2S_3 powders were prepared by reacting Bi and S grains in an
40 evacuated quartz tube at 500 °C for 10 hours. The mixture of starting materials of 0.8 g and CsCl/KCl
41 powder of 8 g was sealed in the evacuated quartz tube. The tube was heated at 800 °C for 10 hours
42 and kept it at 800 °C for 10 hours and cooled down to 630 °C at the rate of 0.3 °C/h or 1 °C/h. After
43 this thermal process, the obtained material was washed by distilled water to remove the flux. X-ray
44 diffraction (XRD) patterns using single crystal and powder samples were collected by a Rigaku X-ray
45 diffractometer with $\text{Cu K}\alpha$ radiation using θ - 2θ method. These powder samples used in XRD

46 measurements were prepared by grinding single crystals. Lattice constants along the a and c axis are
 47 determined by using θ - 2θ technique. Temperature dependence of the magnetic susceptibility down
 48 to 2 K was measured with MPMS (Magnetic Property Measurement System). Temperature
 49 dependence of the electrical resistivity was measured down to 2.5K with four terminals method.

50 3. Result

51 Fig. 1(a) shows X-ray diffraction patterns for $\text{NdO}_{0.7}\text{F}_{0.3}\text{Bi}_{1-x}\text{Sb}_x\text{S}_2$ ($x=0.01-0.10$). All the peaks
 52 correspond to the $(00l)$ peaks of CeOBiS_2 type structure with the space group $P4/nmm$ symmetry. The
 53 (004) peaks of these samples are magnified in Fig. 1(b). The peaks are gradually shifted to high angle
 54 side with increasing the Sb concentration. This is indicative of success in Sb substitution into
 55 $\text{NdO}_{0.7}\text{F}_{0.3}\text{BiS}_2$ up to $x=0.10$. Fig. 1(c) shows a Sb concentration dependence of the lattice constant along
 56 the c axis. The lattice constant is almost constant up to $x=0.04$ and decreases above $x=0.04$. The lattice
 57 constant along the a axis shows almost constant until $x=0.10$ as depicted in Fig. 1 (d). The lattice
 58 shrinkage in both axes by the Sb substitution was caused by the difference of ionic radius between Bi
 59 and Sb ion as we expected. Next, superconducting properties of these samples were evaluated to
 60 investigate an effect of the Sb substitution to the superconductivity.

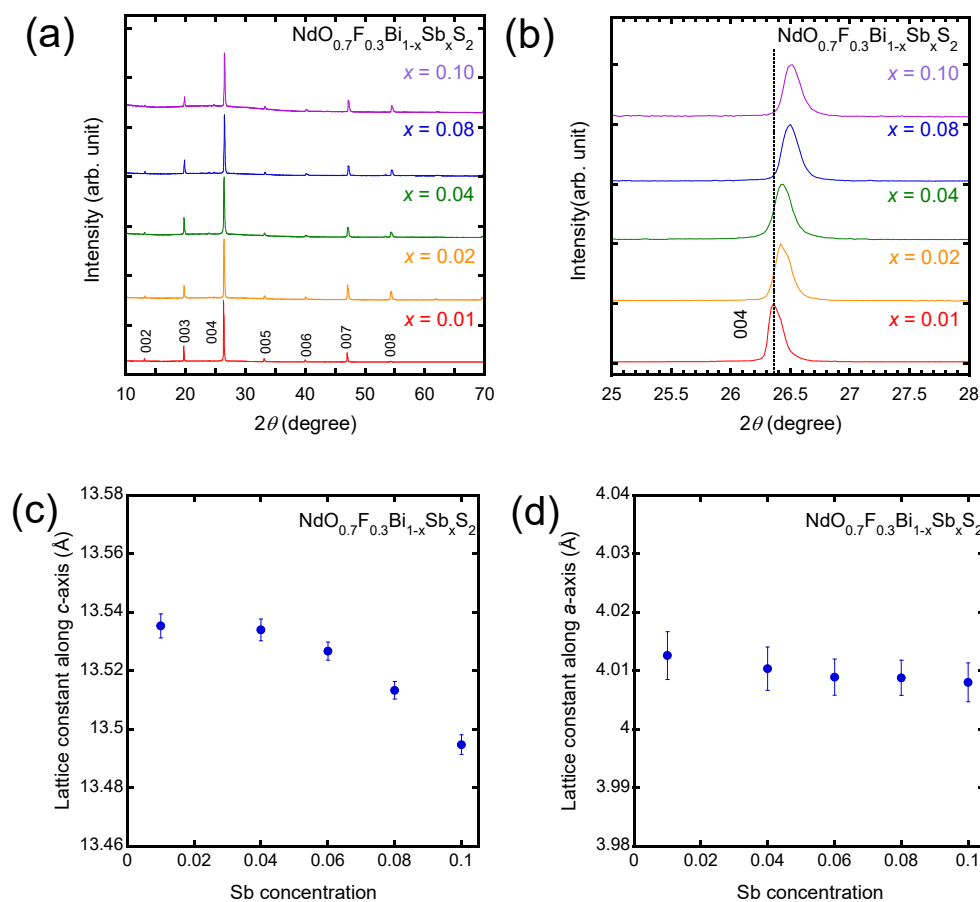


Figure 1. XRD patterns and lattice parameters of $\text{NdO}_{0.7}\text{F}_{0.3}\text{Bi}_{1-x}\text{Sb}_x\text{S}_2$ single crystals. (a) XRD patterns from $x=0.01$ to 0.10 on the $\text{NdO}_{0.7}\text{F}_{0.3}\text{Bi}_{1-x}\text{Sb}_x\text{S}_2$. (b) Magnified figure near (004) peak in Fig. 1(a). (c, d) Lattice constants along the c and a axis for $\text{NdO}_{0.7}\text{F}_{0.3}\text{Bi}_{1-x}\text{Sb}_x\text{S}_2$.

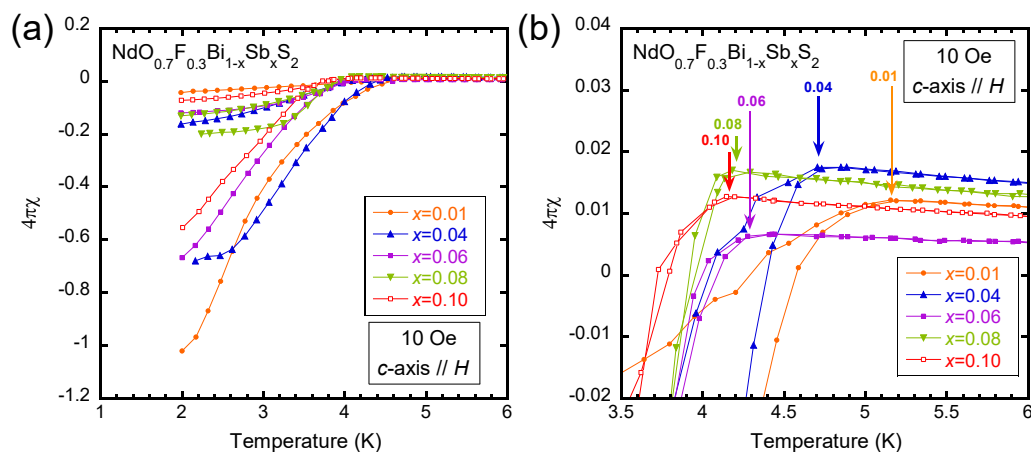


Figure 2. Magnetic susceptibility for $\text{NdO}_{0.7}\text{F}_{0.3}\text{Bi}_{1-x}\text{Sb}_x\text{S}_2$ as a function of Temperature. (a) Temperature dependence of magnetic susceptibility for $\text{NdO}_{0.7}\text{F}_{0.3}\text{Bi}_{1-x}\text{Sb}_x\text{S}_2$ from 1K to 6K. (b) The magnetic susceptibility near the superconducting transition for $\text{NdO}_{0.7}\text{F}_{0.3}\text{Bi}_{1-x}\text{Sb}_x\text{S}_2$.

62 Fig. 2 (a) and (b) show magnetic susceptibility as a function of temperature for $\text{NdO}_{0.7}\text{F}_{0.3}\text{Bi}_{1-x}\text{Sb}_x\text{S}_2$
 63 $(x=0.01-0.10)$ at magnetic field of 10 Oe. All samples show diamagnetic signal due to an
 64 appearance of superconductivity. A magnitude of $4\pi\chi$ decreases from 1 at $x=0.01$ to 0.2 at $x=0.08$, and
 65 increase again to 0.6 at $x=0.10$. In the contrast to the magnitude of $4\pi\chi$, the superconducting transition
 66 temperature (T_c) monotonously decreases with increasing Sb concentration as shown in Fig. 2(b). In
 67 the zero field cooling process, all samples show a broad superconducting transition. This broad
 68 transition is often observed in the other $\text{Ln}(\text{O},\text{F})\text{BiCh}_2$ ($\text{Ln}=\text{La}, \text{Ce}, \text{Pr}, \text{Nd}, \text{Ch}=\text{S}, \text{Se}$) [21-25]. Although
 69 the reason why the transition is broadened has not been known yet, the broad transition is seemed
 70 to be common feature in these materials.

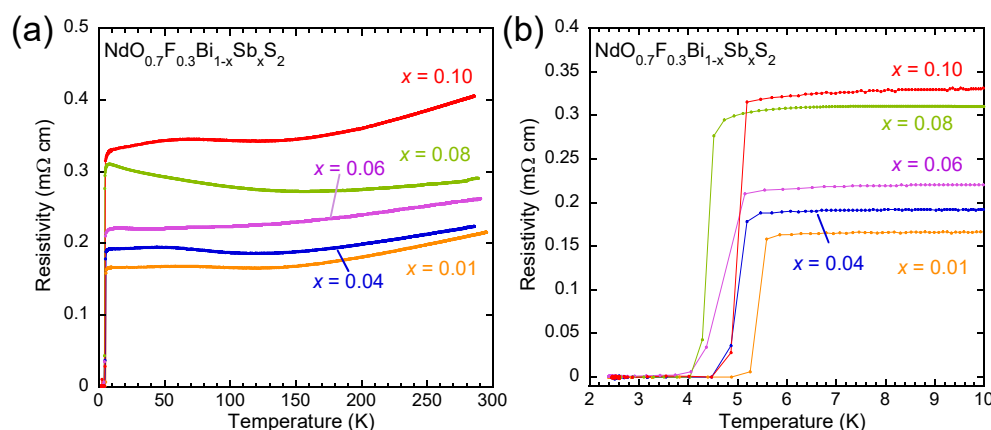


Figure 3. Temperature dependence of electrical resistivity for $\text{NdO}_{0.7}\text{F}_{0.3}\text{Bi}_{1-x}\text{Sb}_x\text{S}_2$. (a) Temperature dependence of electrical resistivity for $\text{NdO}_{0.7}\text{F}_{0.3}\text{Bi}_{1-x}\text{Sb}_x\text{S}_2$ ($x=0.01-0.10$) from 2K to 300K. (b) Temperature dependence of electrical resistivity for $\text{NdO}_{0.7}\text{F}_{0.3}\text{Bi}_{1-x}\text{Sb}_x\text{S}_2$ ($x=0.01-0.10$) from 2K to 10K.

71 Fig. 3 (b) shows the electrical resistivity near T_c as a function of temperature. Steep drop due to
 72 an appearance of superconductivity is observed at around 5.2 K at the sample with $x=0.01$. The
 73 transition temperature decreases with increasing the Sb concentration. At $x=0.10$, T_c slightly recovers
 74 to 5 K. Resistivity at room temperature (RT) continuously increases by Sb substitution as shown in
 75 Fig. 3(a). This is because the Sb ion is substituted for Bi ion located in the conduction layers. This
 76 increase in resistivity at RT is also observed in Pb substituted $\text{Ln}(\text{O},\text{F})\text{BiS}_2$ ($\text{Ln}=\text{La}, \text{Nd}$) [15,16],
 77 whereas Pb substitution induced an enhancement of T_c . Therefore, an effect of the substitution on
 78 superconductivity does not correlate to the strength of the scattering by the substituted atoms.

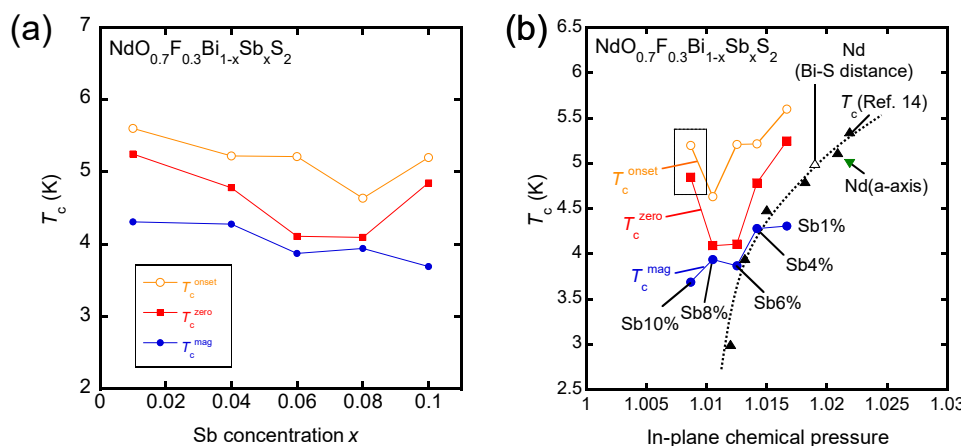


Figure 4. (a) Sb concentration x dependence of T_c for $\text{NdO}_{0.7}\text{F}_{0.3}\text{Bi}_{1-x}\text{Sb}_x\text{S}_2$. (b) Estimated in-plane chemical pressure dependence of T_c for $\text{NdO}_{0.7}\text{F}_{0.3}\text{Bi}_{1-x}\text{Sb}_x\text{S}_2$. T_c of $(\text{Ce},\text{Nd})\text{O}_{0.5}\text{F}_{0.5}\text{BiS}_2$ and $(\text{Nd},\text{Sm})\text{O}_{0.5}\text{F}_{0.5}\text{BiS}_2$ is plotted as the triangles, which is fitted by hand as shown in the dot-line [14].

79 Fig. 4(a) shows a summary of the observed T_c . Here, T_c^{mag} is defined as a temperature at which
 80 magnetic susceptibility begins to decrease. T_c^{onset} and T_c^{zero} are defined as a temperature at which
 81 resistivity begins to decrease and the temperature where resistivity becomes zero. All T_c monotonically
 82 decrease with an increase of the Sb concentration except for $x=0.1$.

83 Mizuguchi et al. reported that T_c of BiCh_2 superconductors is correlated with in-plane chemical
 84 pressure [18]. To compare the result in Sb substituted samples with the previous report, we estimated
 85 in-plane chemical pressure for $\text{NdO}_{0.7}\text{F}_{0.3}\text{Bi}_{1-x}\text{Sb}_x\text{S}_2$. In-plane chemical pressure is defined by the ionic
 86 radius of Bi and chalcogenide ion, and a distance between Bi and chalcogenide ion located in BiCh_2
 87 plane. In the case of Sb substitution, this in-plane chemical pressure is defined as following:

$$88 \quad \text{In-plane chemical pressure} = ((1-x)R_{\text{Bi}} + xR_{\text{Sb}} + R_{\text{Ch}}) / \text{Bi-Ch1 (in-plane) distance}$$

89 where R_{Bi} is an ionic radius of Bi ion. In this study, the ionic radius of Bi ion was obtained from the
 90 structural data of the $\text{LaO}_{0.77}\text{F}_{0.23}\text{BiS}_2$ single crystal [26]. Thus, the value of R_{Bi} was 104.75 pm, which is
 91 the almost same value as that in the previous report [18]. R_{Sb} and R_{Ch} are ionic radii of Sb^{3+} and
 92 Ch^{2-} ions, respectively. These values were determined as 76 and 184 pm from a reference [27]. The Bi-Ch1
 93 distance was estimated by the lattice constant along the a axis in this study. Since the lattice
 94 constant along the a axis corresponds to the length of a side of the Bi square lattice, we use $1/\sqrt{2}$
 95 times of the lattice constant along the a axis as the Bi-Ch1 distance. Fig. 4(b) shows the estimated in-
 96 plane chemical pressure dependence of T_c^{onset} , T_c^{mag} and T_c^{zero} , shown in squares, filled circles and
 97 open circles, respectively. Except for T_c^{onset} and T_c^{zero} in $x=0.10$ sample, T_c of all samples decreases
 98 with the decrease in in-plane chemical pressure. From this result, T_c in the Sb substituted materials
 99 are positively correlated to in-plane chemical pressure. To compare this result and the results in
 100 $\text{Ce}_y\text{Nd}_{1-y}\text{O}_{0.5}\text{F}_{0.5}\text{BiS}_2$ and $\text{Nd}_y\text{Sm}_{1-y}\text{O}_{0.5}\text{F}_{0.5}\text{BiS}_2$ in Ref. 14, T_c of $\text{Ce}_y\text{Nd}_{1-y}\text{O}_{0.5}\text{F}_{0.5}\text{BiS}_2$ and $\text{Nd}_y\text{Sm}_{1-}$
 101 $y\text{O}_{0.5}\text{F}_{0.5}\text{BiS}_2$ were superimposed in Fig. 4(b), which are shown in triangles. T_c in these materials shows
 102 almost close change against in-plane chemical pressure. Thus, our result is qualitatively consistent
 103 with the previous results in Ref. 14. In addition, these results suggest the concept of in-plane chemical
 104 pressure is valid in the case of substitution not only at Ln site in the blocking layer, but also at Bi site
 105 in the conduction layer.

106 In this study, the in-plane chemical pressure is estimated by the lattice constant along a axis. On
 107 the other hand, the in-plane chemical pressure in Ref. 14 is estimated by the Bi-Ch1 distance obtained
 108 by the data of the single crystal analysis. To compare the difference of these estimated in-plane
 109 chemical pressure, both value is estimated by using the data of the single crystal analysis the Ref. 28.
 110 the in-plane chemical pressure estimated by the Bi-Ch1 distance is plotted as open triangle, while
 111 that estimated by the a axis is plotted as the inversed triangle in Fig. 4(b). The later one slightly has
 112 the higher value in comparison with the former one. However, since this value is located at the

113 extrapolated line of the T_c of Sb-substituted samples, this estimation is reasonable to estimate the in-
 114 plane chemical pressure qualitatively.

115 T_{c}^{onset} and T_{c}^{zero} in $x=0.10$ sample determined by electric resistivity measurements deviate
 116 from the T_c vs. in-plane chemical pressure relation in other samples. One possible reason of this result
 117 is the distribution of the Sb concentration. An electrical resistivity measurement is sensitive to high
 118 conductivity pass showing the highest T_c even though such a region is quite small. In this study, T_c
 119 decreases with increasing the Sb concentration. Therefore, the minor region with the low Sb
 120 concentration is expected to coexist with the major region with the high Sb concentration. To reveal
 121 this deviation and the expectation, the further spatial composition analysis is needed.

122 Finally, we compare this effect of the Sb substitution with the effect of the Pb substitution in
 123 $\text{NdO}_{0.7}\text{F}_{0.3}\text{BiS}_2$ because this Pb ion is expected to be substituted into Bi site. The Sb substitution
 124 suppresses the superconductivity. This suppression is understood by the decrease of the in-plane
 125 chemical pressure described by this paper. On the other hand, Pb substitution increases T_c up to 6 K.
 126 The in-plane chemical pressure of Pb substituted samples is almost constant because an ionic radius
 127 of Pb^{2+} ion is almost same as that of $\text{Bi}^{2.7}$ ion calculated by the single crystal analysis. The ionic radius
 128 of Pb^{2+} ion is 100 pm [29]. If Pb ion is substituted until $x=0.10$, $R_{\text{Bi}}+R_{\text{Pb}}$ is around 103.8 pm which is
 129 almost same value of the ionic radius of $\text{Bi}^{2.7}$ ion of 104.75 pm. This indicates T_c of Pb substituted
 130 samples is independent with the value of the in-plane chemical pressure.

131 4. Summary

132 The examination of Sb substitution less than 10 % is performed on $\text{NdO}_{0.7}\text{F}_{0.3}\text{BiS}_2$. The Sb
 133 substitution caused the decrease in lattice constants along the a and the c axis, and the decrease in T_c
 134 and superconducting volume fraction. The deterioration by these superconducting properties by the
 135 partial Sb substitution into Bi site is explained in terms of the decrease of the in-plane chemical
 136 pressure, indicating of the usefulness of in-plane chemical pressure in BiCh_2 superconductor.

137 **Acknowledgements:** This work was partly supported by a Grant-in-Aid for Young Scientists (B) (No. 15K17710)
 138 and the Nanotech Career-up Alliance (Nanotech CUPAL).

139 References

- 140 1 Y. Mizuguchi, H. Fujihisa, Y. Gotoh, K. Suzuki, H. Usui, K. Kuroki, S. Demura, Y. Takano, H. Izawa, O.
 141 Miura, *Phys. Rev. B* 86 (2012) 220510(R).
- 142 2 S. K. Singh, A. Kumar, B. Gahtri, G. Sharma, S. Patnaik, and V. P. S. Awana, *J. Am. Chem. Soc.*, 13416504
 143 (2012).
- 144 3 Y. Mizuguchi, S. Demura, K. Deguchi, Y. Takano, H. Fujihisa, Y. Gotoh, H. Izawa, O. Miura, *J. Phys. Soc.*
 145 *Jpn.* 81 (2012) 114725.
- 146 4 V. P. S. Awana, Anuj Kumar, Rajveer Jha, Shiva Kumar Singh, Anand Pal, Shruti, J. Saha, S. Patnaik, *Solid*
 147 *State Commun.*, 157, 21 (2013).
- 148 5 S. Demura, Y. Mizuguchi, K. Deguchi, H. Okazaki, H. Hara, T. Watanabe, S. J. Denholme, M. Fujioka, T.
 149 Ozaki, H. Fujihisa, Y. Gotoh, O. Miura, T. Yamaguchi, H. Takeya, Y. Takano, *J. Phys. Soc. Jpn.* 82 (2013)
 150 033708.
- 151 6 R. Jha, A. Kumar, S. K. Singh, and V. P. S. Awana, *J. Appl. Phys.* 113, 056102 (2013).
- 152 7 J. Xing, S. Li, X. Ding, H. Yang, H. Wen, *Phys. Rev. B* 86 (2012) 214518.
- 153 8 R Jha, A. Kumar, S. K. Sng, V. P. S. Awana, *J. Sup. and Novel Mag.* 26, 499-502 (2013).
- 154 9 D. Yazici, K. Huang, B. D. White, I. Jeon, V. W. Burnett, A. J. Friedman, I. K. Lum, M. Nallaiyan, S. Spagna,
 155 M. B. Maple, *Phys. Rev. B* 87 (2013) 174512.
- 156 10 J. Kajitani, A. Omachi, T. Hiroi, O. Miura, Y. Mizuguchi, *Physica C* 504 (2014) 33-35.
- 157 11 T. Hiroi, J. Kajitani, A. Omachi, O. Miura, Y. Mizuguchi, *J. Phys. Soc. Jpn.* 84 (2015) 024723.
- 158 12 Y. Fang, D. Yazici, B. D. White, M. B. Maple, *Phys. Rev. B* 91 (2015) 064510.
- 159 13 D. Yazici, I. Jeon, B.D. White, M.B. Maple, *Physica C*, 514, p. 218-236.
- 160 14 Y. Fang, C. T. Wolowiec, D. Yazici, M. B. Maple, *Nov. Supercond. Mater.* 1, 79-94 (2015).
- 161 15 S. Demura, Y. Fujisawa, S. Otuski, R. Ishio, Y. Takano, H. Sakata *Solid State Communications* 223 (2015)
 162 40-44.

- 163 16 S. Demura et al, in preparation
164 17 S. Demura, *Nov. Supercond. Mater.* 2, 1-15 (2016).
165 18 Y. Mizuguchi, A. Miura, J. Kajitani, T. Hiroi, O. Miura, K. Tadanaga, N. Kumada, E. Magome, C. Miriyoshi,
166 19 Y. Kuroiwa, *Scientific Reports* 5, Article number: (2015) 14968.
167 20 M. Nagao, A. Miura, S. Demura, K. Deguchi, S. Watauchi, T. Takei, Y. Takano, N. Kumada, I. Tanaka *Solid*
168 21 *State Commun.* 178 (2014) 33–36.
169 22 M. Nagao, *Nov. Supercond. Mater.* 1, 64-74 (2015).
170 23 S. Otski, S. Demura, Y. Sakai, Y. Fujisawa, and H. Sakata. *Solid State Commun.*, in Press.
171 24 A. Miura, M. Nagao, T. Takei, S. Watauchi, Y. Mizuguchi, Y. Takano, I. Tanaka, and N. Kumada, *Cryst.*
172 25 *Growth Des.* 15, 39 (2015).
173 26 M. Nagao, A. Miura, S. Watauchi, Y. Takano and I. Tanaka, *Jpn. J. Appl. Phys.* 54, 083101 (2015).
174 27 M. Nagao, S. Demura, K. Deguchi, A. Miura, S. Watauchi, T. Takei, Y. Takano, N. Kumada, and I. Tanaka,
175 28 *J. Phys. Soc. Jpn* 82, 113701 (2013).
176 29 M. Tanaka, M. Nagao, Y. Matsushita, M. Fujioka, S. J. Denholme, T. Yamaguchi, H. Takeya, and Y. Takano,
177 30 *J. Solid State Chem.* 219, 168 (2014).
178 31 A. Miura, M. Nagao, T. Takei, S. Watauchi, and I. Tanaka, *J. Solid State Chem.* 212 213 (2014).
179 32 Y. Q. Jia, *J. Solid State Chem.* 95, 184 (1991).
180 33 M. Nagao, S. Demura, K Deguchi, A. Mura, S Watauchi, T. Takei, Y. Takano, N. Kumada, and I. Tanaka, *J.*
181 34 *Phys. Soc. Jpn.* 82 113801 (2013).
182 35 S. Demura, Y. Fujisawa, S. Otuski, R. Ishio, Y. Takano, H. Sakata *Solid State Communications* 223 (2015)
183 36 40-44.